

Neutron Interferometric Measurement of Neutron Pair Correlations for Multiple Detectors

David L. JACOBSON, Brendan.E. ALLMAN, *Michael ZAWISKY, Samuel A. WERNER and *Helmut RAUCH

Physics Department and Research Reactor Center, University of Missouri-Columbia, Columbia, Missouri 65211, USA.

**Atominstytut der Österreichischen Universitäten, Schüttelstrasse 115, A-1020 Wien, Austria.*

(Received 1 February 1996; accepted 7 July 1996)

We have experimentally measured the cross-correlation of neutron arrival times in the detectors of a neutron interferometer. A comparison of the experimental results is made for both a chopped and un-chopped incident neutron beam. The experimentally detected cross-correlations are presented and compared with the theory based on the Poissonian statistics of truly random events. By varying the neutron interferometric phase we look for quantum effects in the cross-correlations which are not explainable by the classical Poissonian statistical theory. We have also placed 57% efficient detectors, which are virtually phase transparent, inside the interferometer (in addition to the standard 99% absorption detectors in the exit beams).

KEYWORDS: Pair Correlation, Chopper, Neutron Interferometry

1. Introduction

Recent neutron interferometry experiments¹⁻⁶⁾ have measured the neutron coherence effects described by the auto-correlation function^{7,8)}

$$\Gamma^{(1)}(\Delta, \tau = 0) = \langle \Psi(0,0)^* \Psi(\Delta,0) \rangle, \quad (1)$$

where Δ is the spatial delay of the neutron wave packet. These experiments measured the longitudinal, vertical and transverse coherence lengths ($50\text{\AA} \times 200\text{\AA} \times 50,000\text{\AA}$).

The coherence time may be calculated from $\tau^c = \Delta^c / v_0$ where Δ^c is the coherence length and v_0 (~ 2000 m/s) is the group velocity of the wave packet. This calculation gives a value of $\sim 10^{-12}$ s as the expected coherence time. Such a small coherence time is well beyond the uncertainty limit ($\sim 10^{-6}$ s) imposed by current neutron detection technology. It is then expected that the mutual coherence function, for neutron pairs, reduces to the classical pair correlation function for randomly arriving neutrons⁷⁻⁹⁾, i.e.,

$$\Gamma_{a \rightarrow b}^{(2)}(\Delta, \tau) = \langle I_a(0,0) I_b(\Delta, \tau) \rangle. \quad (2)$$

In Eq. (2) "a" and "b" distinguish two different detectors. Previous experiments have examined the case when a and b are the same detector¹⁰⁾. In this experiment we are interested in correlating pairs, in separate detectors (i.e., $a \neq b$), on a time scale which is on the same order as the detector temporal resolution ($\sim 5\mu\text{s}$) to see if theory and experiment match.

This experiment was performed at the University of Missouri Research Reactor Center on the beam port C interferometry station which operates at a fixed nominal wavelength $\lambda = 2.35\text{\AA}$ ($v = 1.683\text{mm}/\mu\text{s}$). This interferometer setup has the advantage of high flux and good long-term stability.

In addition to the standard 99% efficient O and H beam detectors we have placed two detectors with roughly 57% efficiency inside the back half of the interferometer (see Fig.1). By wrapping these detectors with titanium, which has a negative scattering length, we exploited the neutron

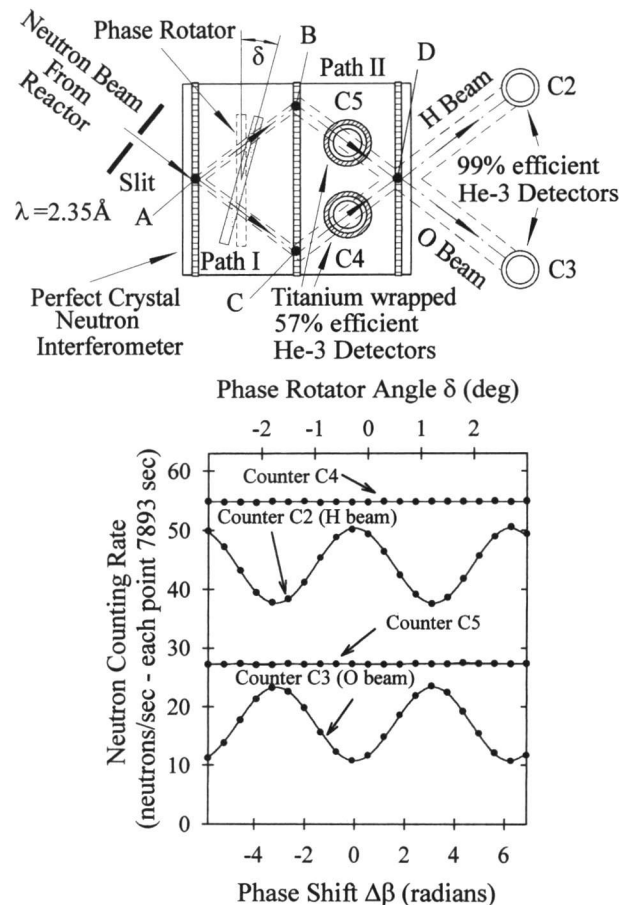


Fig. 1. The experimental setup used in this experiment is shown in the top panel. In the above figure a perfect silicon crystal interferometer (distance between blades=5cm, blade thickness =0.35cm) splits a beam of neutrons which has passed through a 4mm \times 10 mm slit near at point "A". At points B and C the beams are reflected so that they travel through two 57% efficient He-3 detectors to meet at point D. The outgoing beams after point D are coherent linear combinations of the wave function after having traversed paths I and II. An aluminum slab extends across both beams to allow the relative phase shift between the two paths to be varied. The lower panel shows the variation of intensity for the four detectors as the aluminum slab is rotated.

phase echo effect to render these detectors virtually phase transparent⁴⁾.

2. Un-Chopped Experiment

In the first part of this experiment the arrival times of neutrons in the detectors are measured. After correcting for the time-of-flight between the separate detectors (10^5 - $10^9\mu\text{s}$) it will be shown how the neutrons are distributed in time between the individual detectors.

The O and H beam intensities are functions of the relative phase difference $\Delta\beta$ between the neutron wave which traverses path II and the wave which travels path I. The O and H beam intensities are given by^{11,12)}

$$I_O = \bar{I}_O \left(1 + C_i \cos(\Delta\beta(\delta) + \Delta\beta_0)\right), \quad (3a)$$

$$I_H = \bar{I}_H - \bar{I}_O C_i \cos(\Delta\beta(\delta) + \Delta\beta_0), \quad (3b)$$

where \bar{I}_O is the average counting rate in the O beam, \bar{I}_H is the average counting rate in the H beam, $\Delta\beta(\delta)$ is the phase shift due to the aluminum phase rotator flag and $\Delta\beta_0$ is the offset phase shift (empty interferometer) between path II and path I. The intensity in the detectors inside the interferometer are expected to be constant as $\Delta\beta(\delta)$ is varied. These single particle intensity variations are recorded in order to separate them from any anomalous two particle intensity correlations.

The initial contrast C_i is defined by the minimum and maximum counting rates in C2 and C3, i.e.,

$$C_i = \frac{I_{\max} - I_{\min}}{I_{\max} + I_{\min}}. \quad (4)$$

The initial contrast is less than unity due to imperfections in the interferometer crystal, vibration in the experimental setup, and unavoidable density variations across the transmission detectors inside the interferometer.

To correlate all four detectors, it is necessary to develop a theory to describe the probability of counting a neutron at a time $t+\tau$, in any one of the four detectors, after having counted a previous neutron in one of the detectors at a time t . It will be assumed that the neutrons from the reactor arrive at random times in the detectors. For randomly arriving neutrons the probability $p=I\Delta t$ represents the probability of measuring a neutron in a time interval Δt . It is required that p be constant and that $p \ll 1$ which may easily be guaranteed by picking Δt appropriately small. The probability of detecting a neutron in detector "b" at a time $\tau=n\Delta t$ later after having measured a neutron in detector "a" at a time t is then

$$W_n = \left(\begin{array}{l} \text{Probability of not measuring a neutron} \\ \text{between times } t \text{ and } t+\Delta t \text{ in detector "a"} \end{array} \right) \\ \times \left(\begin{array}{l} \text{Probability of finally measuring only one} \\ \text{neutron at a time } t+\Delta t \text{ later in "b"} \end{array} \right) \quad (5) \\ = \left[(1-p_a)^n \right] \times \left[(1-p_b)^{n-1} p_b \right],$$

where $p_a=I_a\Delta t$, $p_b=I_b\Delta t$ and n is an integer greater than or equal to 1. Using Eq. (5) the neutron pair probability

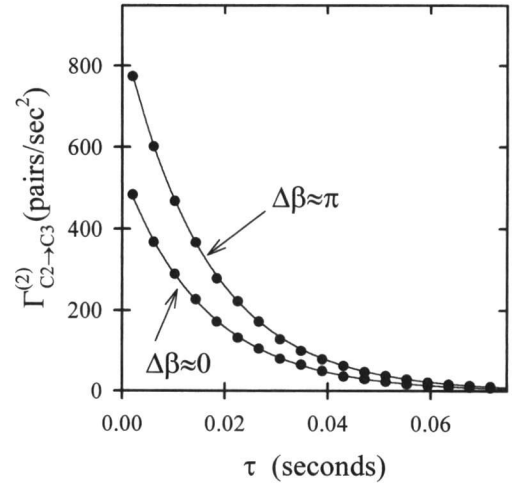


Fig. 2. The pair correlation function for neutrons detected in detector C2 and C3 for two different phase shifts $\Delta\beta$. Each point is the average number of pairs per second detected in an interval $\Delta t=4.1\text{ms}$. The solid line represents a fit to Eq. (7).

density for $a \neq b$ may be written as

$$W_{a \rightarrow b}(\Delta\beta, \tau) = \lim_{\Delta t \rightarrow 0} \frac{W_n}{\Delta t} \quad (6) \\ = I_b(\Delta\beta) e^{-(I_a(\Delta\beta) + I_b(\Delta\beta))\tau},$$

which is a decaying exponential in pair spacing time τ .

The pair correlation function is the product of the intensity in detector "a" and the neutron pair probability function

$$\Gamma_{a \rightarrow b}^{(2)}(\Delta\beta, \tau) = I_a(\Delta\beta) W_{a \rightarrow b}(\Delta\beta, \tau). \quad (7)$$

In Fig.2 the data collected when a is detector C2 and b is detector C3 is plotted along with Eq. (7).

The data plotted in Fig.2 were measured by recording the time of arrival of each neutron using four Ortec MCS II cards which were plugged into the bus slots of a Hewlett Packard 486 PC. The MCS cards were used to count the number of clock pulses (pulse period = $0.820\mu\text{s}$) between neutron arrivals. By counting clock pulses the absolute time of arrival of each neutron was recorded.

In this experiment the neutrons which arrive with small pair spacing time τ are examined since these neutrons are the most likely to exhibit anomalous correlations. Summing the pairs arriving per second for pair spacings between 0 and, say, τ_2 gives

$$I_{a \rightarrow b}(\Delta\beta) = \int_0^{\tau_2} \Gamma_{a \rightarrow b}^{(2)}(\Delta\beta, \tau) d\tau \\ = I_a(\Delta\beta) I_b(\Delta\beta) \tau_2 \frac{[1 - e^{-(I_a(\Delta\beta) + I_b(\Delta\beta))\tau_2}]}{(I_a(\Delta\beta) + I_b(\Delta\beta))\tau_2}. \quad (8)$$

It is necessary to focus on neutrons arriving at time scales greater than the detection time uncertainty ($\sim 5\mu\text{s}$), and so a comparable time scale of $41\mu\text{s}$ was chosen. This time scale is also comparable to the time-of-flight across the interferometer which is $77\mu\text{s}$. In Fig.3 the data are plotted along with Eq. (8) for this time scale as a function of the relative single particle phase difference $\Delta\beta$. By varying the

single particle phase shift via the phase shifter, the intensity loss or gain due to single particle correlations are distinguished from the intensity differences due to unexpected, two particle correlations. Neutrons arriving in the detectors appear to be randomly distributed with no correlation effects beyond those predicted by classical Poissonian statistics.

3. Chopped Experiment

A Fermi chopper was added to the experimental setup as is shown in Fig.4. This chopper was incorporated into the experimental setup in order to look for anomalous correlations between any two neutrons localized in a chopped pulse.

This chopper was built by the URANIT Corporation and was operated at a rotational frequency $f=30,000$ rpm. The chopper wheel has 12 equally spaced slits which are 1° wide. The chopper creates pulses when the moving slits pass a stationary slit. At 30,000 rpm the full width at half maximum of these pulses is around $5.6 \mu\text{s}$ at the chopper, spreading out downstream at detector C4 to $6.5 \mu\text{s}$.⁶⁾ Each pulse is separated from the next by a $166.7 \mu\text{s}$ flight time.

To describe the chopped data a probability relation similar to Eq. (6) will be derived in which it will be assumed that neutrons are arriving randomly at the chopper from the reactor. These pulses then travel into the interferometer where each detector has a certain probability of detecting a neutron within the pulse depending on the counting rate in the detector. For a triangular shaped chopper pulse shown in Fig.5, the probability of measuring a neutron at any time t is given by

$$p(t) = \bar{I}\Delta t \begin{cases} 0; & |\delta t| \geq t_c \\ 1 + \delta t/t_c; & t < 0 \\ 1 - \delta t/t_c; & t \geq 0, \end{cases} \quad (9)$$

where $\delta t = t - t_0$ and t_0 is the center of the chopper pulse, t_c is the full width at half maximum of the chopper pulse at the detector, and \bar{I} is the average counting rate when the beam is not chopped (this rate is much less than the rates shown in Fig.1 due to the small slit used on the chopper). The probability of measuring a neutron in detector "b" at a time $t+\tau$, after measuring a previous neutron in detector "a" is given by (as before)

$$W_{n,a \rightarrow b}^c(t) = \left[\prod_{j=1}^{j=n} (1 - p_a(t + j \cdot \Delta t)) \right] \times \left[\prod_{j=1}^{j=n-1} (1 - p_b(t + j \cdot \Delta t)) p_b(t + \tau) \right], \quad (10)$$

where the superscript c is used to distinguish the chopped and un-chopped probability functions. Since $(I_a + I_b)\tau \ll 1$ eq. (10) simplifies to

$$W_{a \rightarrow b}^c(t, \tau) \approx I_b(\Delta\beta, t + \tau) \Delta t e^{-\sum_{j=1}^{j=n} (I_a(t + j\Delta t) + I_b(t + j\Delta t)) \Delta t}, \quad (11)$$

or in terms of the neutron pair probability density

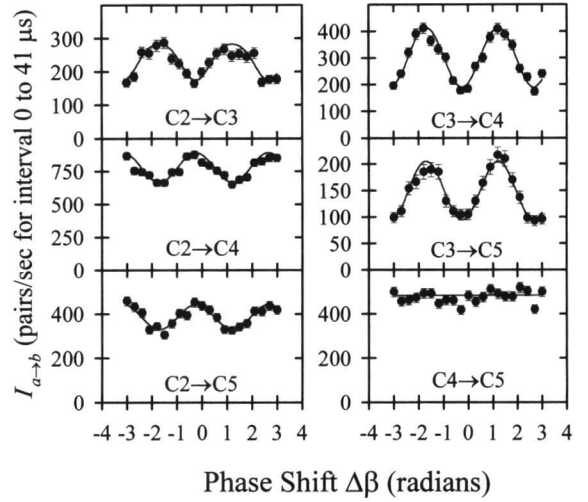


Fig. 3. The average pair correlation function is plotted for arrival times between $\tau=0$ and $\tau=41\mu\text{s}$ as a function of the spatial phase shift. The solid line is the theoretical value based on Eq. (8).

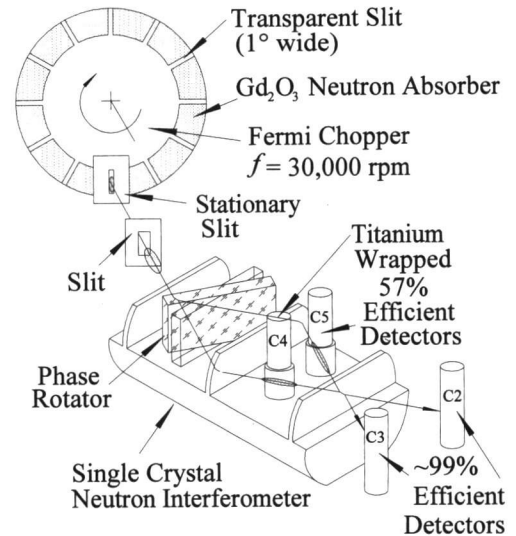


Fig. 4. The placement of a Fermi chopper relative to the interferometer is shown. The stationary slit on the chopper is a $1.5\text{mm} \times 20\text{mm}$ slit which matches the size of the 1° slits on the chopper wheel. On the interferometer is $4\text{mm} \times 10\text{mm}$ slit.

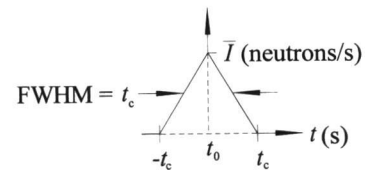


Fig. 5. The shape of a triangular intensity pulse created by the chopper.

$$\begin{aligned}
W_{a \rightarrow b}^c(t, \tau) &= \lim_{\Delta t \rightarrow 0} W_{n, a \rightarrow b}^c / \Delta t \\
&= I_b(\Delta\beta, t + \tau) e^{-\int_t^{t+\tau} dt' (I_a(t') + I_b(t'))} \quad (12) \\
&\approx I_b(\Delta\beta, t + \tau),
\end{aligned}$$

where the fact that the pulse width is small was used. Equation (12) represents the probability density for detecting a neutron in detector "b" at a time $t + \tau$, after having detected a previous neutron in detector "a" at a time t .

The chopper pair correlation function is then

$$\Gamma_{a \rightarrow b}^{(2)c}(\Delta\beta, t, \tau) = I_a(\Delta\beta, t) I_b(\Delta\beta, t + \tau). \quad (13)$$

Instead of recording the time of arrival of neutrons in the chopped pulses, the total number of neutrons in each pulse are counted and stored sequentially in the MCS II cards mentioned in Section 2. Most pulses do not contain any neutrons; however, a very small percentage of the pulses contain one neutron and even fewer contain two neutrons. Pulses with two neutrons allowed multiple detectors to be correlated. Since the detection system is not capable of distinguishing between arrival times t and pair spacings τ it is necessary to sum over all pair spacings τ , and average over all arrival times t in Eq. (15) to achieve the pair counting rate

$$I_{a \rightarrow b}^c(\Delta\beta) = \frac{1}{30 t_c} \int_0^\infty d\tau \int_{-15t_c}^{15t_c} dt \Gamma_{a \rightarrow b}^{(2)c}(\Delta\beta, \tau), \quad (14)$$

where the factor 30 comes from averaging 12 slits around the 360 degrees on the chopper wheel. Substituting the triangular shaped pulse of Eq. (9) into Eq. (14) gives

$$I_{a \rightarrow b}^c(\Delta\beta) = \bar{I}_a(\Delta\beta) \bar{I}_b(\Delta\beta) (t_c / 72), \quad (15)$$

which is plotted with the experimental data in Fig. 6.

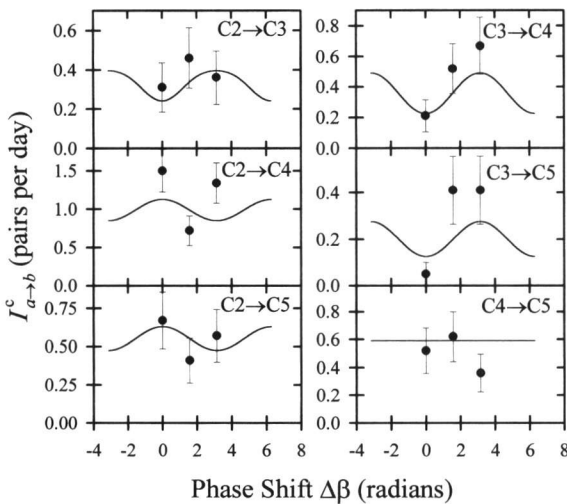


Fig. 6. The data taken for the chopped pair correlation experiment. The cross correlated detectors "a" and "b" are indicated in the upper right hand corner of each plot. The solid line represents the theoretical prediction based on Eq. (15). These data represent the highest resolution for neutron pair correlations achieved in this experiment.

4. Conclusion

The neutron pair correlations have been examined for a Poissonian source of neutrons. The same results obtained in Eqs. (5)-(7) can be obtained without the use of an interferometer by considering the counting statistics of a particle beam. However, the use of a neutron interferometer is unique in that there are no guarantees that pair correlations in a neutron interferometer will be the same as those observed in a particle beam, until such a fact has been demonstrated experimentally. The results of this experiment show that the two are equivalent for pairs separated by currently resolvable flight times.

The un-chopped data agree with what is expected for randomly arriving neutrons separated in time by the detector temporal resolution of $\sim 5 \mu\text{s}$. The chopped data agree qualitatively with the theory of randomly arriving neutrons in that the counting rate is not higher or lower than expected based on Poissonian statistics. However, low counting statistics limits the accuracy of the chopped data. To significantly improve the quality of the chopped data, it is necessary to count for a longer period (e.g. a year). The intensity and temporal resolution could be improved, without the use of a chopper, if faster detectors are used instead.

To perform correlation experiments in which quantum mechanical anti-bunching effects are expected to be observable, a higher neutron flux source and greater detector time resolution are necessary. Experiments using detectors capable of resolving pair spacings on the order of 10^{-12} s, with current neutron flux rates, would be hampered by extremely low counting statistics, even if this time resolution could be achieved. From Eq. (8) we can estimate with the parameters used in this paper, that we could expect on average, to measure only one pair spaced within the ensemble, longitudinal coherence time every 30 years.

One of us (D.L.J.) would like to acknowledge the useful discussions with Yuji Hasegawa (Wien). We would also like to acknowledge support from NSF, Physics Division Grant No. 9024608; Fond zur Förderung der Wissenschaftlichen Forschung (Projekt No. P8456).

- 1) H. Kaiser, S. A. Werner, E. A. George, *Phys. Rev. Lett.* 50, 560 (1983).
- 2) H. Rauch, E. Seidl, D. Tuppinger, D. Petrascheck and R. Scherm, *Zeit. Phys.* B69, 313 (1987).
- 3) S.A. Werner, R. Clothier, H. Kaiser, H. Rauch and H. Wölwitsch, *Phys. Rev. Lett.* 67, 683 (1991).
- 4) R. Clothier, H. Kaiser, S. A. Werner, H. Rauch and H. Wölwitsch, *Phys. Rev.* A44, 5357 (1991).
- 5) H. Kaiser, R. Clothier, S. A. Werner, H. Rauch and H. Wölwitsch, *Phys. Rev.* A45, 31 (1992).
- 6) H. Rauch and H. Wölwitsch, R. Clothier, H. Kaiser, S. A. Werner, *Phys. Rev.* A46, 49 (1992).
- 7) M. Born and E. Wolf, *Principles of Optics* (Pergamon Press, New York 1980).
- 8) L. Mandel and E. Wolf, *Rev. Mod. Phys.* 37, 231 (1965).
- 9) L. Goldberger, H. W. Lewis and K. M. Watson, *Phys. Rev.* 132, 2764 (1963).
- 10) M. Zawisky, H. Rauch and Y. Hasegawa, *Phys. Rev.* A50, 5000 (1994).
- 11) *Neutron Interferometry*, edited by U. Bonse and H. Rauch, (Clarendon, Oxford, 1979).
- 12) S.A. Werner and A. G. Klein, *Methods of Experimental Physics* (Academic, New York, 1986), Vol. 23 Part A, p. 259.